

Communication

# Water Inrush Hazards in the Chaoyang Tunnel, Guizhou, China: A Preliminary Investigation

Nan Zhang <sup>1</sup>, Qian Zheng <sup>2</sup>, Khalid Elbaz <sup>2,3,\*</sup>  and Ye-Shuang Xu <sup>1,\*</sup> 

<sup>1</sup> State Key Laboratory of Ocean Engineering, Department of Civil Engineering, School of Naval Architecture, Ocean, and Civil Engineering, Shanghai Jiao Tong University, Shanghai 200240, China; nan\_zhang@sjtu.edu.cn

<sup>2</sup> Department of Civil and Environmental Engineering, College of Engineering, Shantou University, Guangdong 515063, China; 18hzheng3@stu.edu.cn

<sup>3</sup> Key Laboratory of Intelligence Manufacturing Technology, Ministry of Education, Shantou University, Shantou, Guangdong 515063, China

\* Correspondence: khalid@stu.edu.cn (K.E.); xuyeshuang@sjtu.edu.cn (Y.-S.X.); Tel.: +86-754-8650-4551 (K.E.)

Received: 18 March 2020; Accepted: 6 April 2020; Published: 10 April 2020



**Abstract:** This paper reports on a water inrush hazard, which occurred during the construction of the Chaoyang tunnel in Libo County, Guizhou Province, China. On 10 June 2018, a continuous water inflow of about 57 thousand m<sup>3</sup> of water within 40 min took place at the tunnel excavation face, resulting in three casualties. The objectives of this study are to investigate and discuss the water inrush process of this atypical case. Further, an inclusive description of the implemented emergency responses will be provided. The principal causes of this tunneling incident include the karst geological condition at the construction field, hydraulic conductivity induced by the connection between karst water system and surface water body, and effects of excavation and precipitation. Moreover, based on a preliminary investigation and analysis, three main control measures to overcome similar incidents in the future are proposed: (1) Performing “water inrush risk grading” in areas prone to water inrush; (2) undertaking comprehensive geological forecast for a synthetic analysis; and (3) employing a monitoring system during the construction, and educating workers on self-protection skills. These effective management measures are bound to benefit underground engineering constructions with regard to water inrush risks.

**Keywords:** water inrush; Libo; fatal accidents; control measures

## 1. Introduction

With the rapid economic growth and continuous urbanization process, an overwhelming number of infrastructure projects has been carried out in China over the past 30 years [1–4]. In the construction process of these infrastructures and facilities, many human engineering activities including tunneling [5–9], dewatering [10–19], excavations [20–23], and embankment constructions [24–27] have resulted in disastrous hazards and fatal incidents. These hazards can occur in inland areas [28–30] as well as coastal areas [31–36]. For instance, on 21 January 2006, an unprecedented water inrush incident happened during the construction of the Malujing tunnel in the Enshi Prefecture, Hubei Province, causing 11 casualties and many injuries [37]. A similar geohazard occurred in Hubei Province on 5 August 2007, resulting in 3 casualties and 19 injuries [38].

This paper presents a preliminary investigation of a water inrush incident in Libo County, Guizhou Province. First, the engineering background of the project is presented, followed by a methodical description of the water inrush incident and rescue operation. The potential causes of the water inrush hazard are thoroughly discussed. Finally, effective management measures for water inrush risks are proposed.

## 2. Background

Libo County is located in the southeast of Guizhou Province in China, as shown in Figure 1. The Chaoyang railway tunnel is a part of the Guiyang–Nanning High-speed Railway Project, which represents a key section of the “China’s Medium- and Long-term Railway Network Plan 2016”. With a total investment of 75.8 billion CNY (11.4 billion US \$), The Guiyang–Nanning High-Speed Railway Project is designed to achieve a running speed of 350 km/h and transportation capacity of 40 million people per year. There are 11 stations along the line from Longli North Railway Station in Guangxi province to Nanning Dong Railway Station in Guizhou province. The overall length of the project covers 512 km of which 483 km are newly constructed.

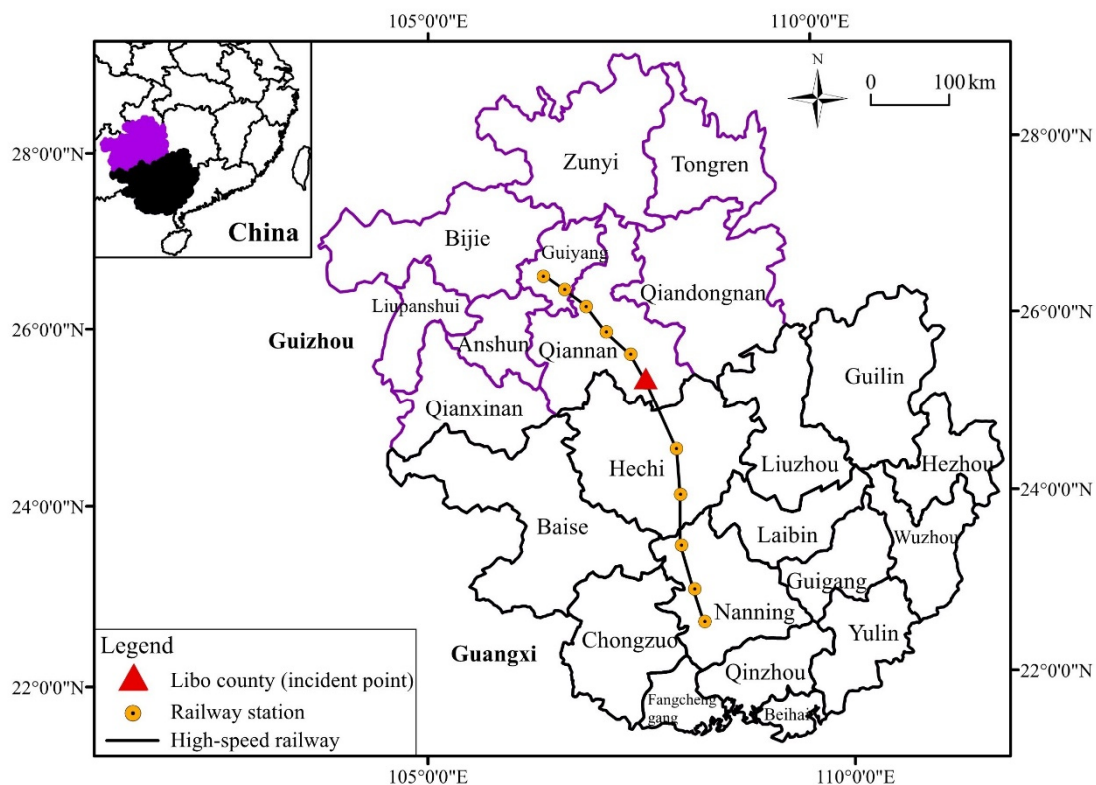


**Figure 1.** Location of water inrush incident along project line.

The Chaoyang railway tunnel project exhibits approximately 12,734 m in length with a maximal buried depth of 386 m. The tunnel line passes through a complex geological profile characterized by the transition zone between limestone mountain (Qiangui plateau) and peak forest-plain area (western Guangxi). Indeed, dense vegetation is observable at the surface of the tunnel in this area. More importantly, the geological investigations revealed the presence of karst geology, which typically hampers tunnel construction processes. Given this challenge and in order to reduce the construction time, a short excavation method was employed in the tunneling process; in particular, four service galleries including two parallel holes, two transverse holes, and an inclined shaft were equipped for drainage during the construction and operation period. Nevertheless, the water inrush incident occurred at the tunnel face located 1893 m away from the structural opening (see Figure 2).

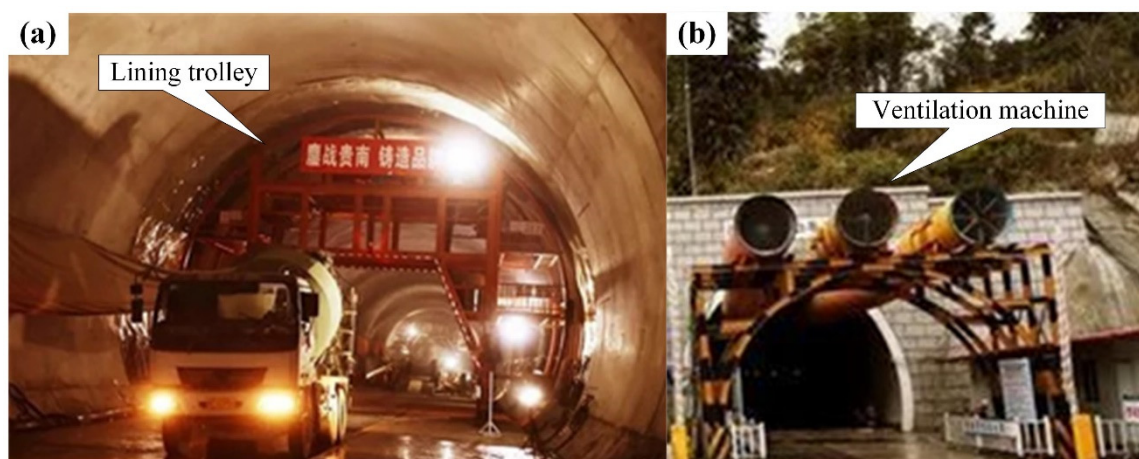


**Figure 2.** Construction situation (a) inside and (b) outside the tunnel before the incident.

### 3. Water Inrush Incident and Rescue Operation

#### 3.1. Water Inrush Incident

At 4:40 a.m. on 30 May 2018, a muddy water ejection from the bottom plate with increasing pressure occurred during the drilling operations on the tunnel face. As a result, the excavation was temporarily stopped, and exploratory drilling was conducted to decipher the geologic conditions and trend of the water-eroded groove in front of the tunnel face. The surrounding rocks of the tunnel face were observed daily to ensure the stability of future excavation operations. Nevertheless, at 8:30 a.m. on 10 June 2018, a non-pressure water leakage was found at the early inrush points in the tunnel face. At 9:56 a.m., a heavy flood of water and mud suddenly ejected out (as shown in Figure 3), and the water level reached a maximal height of 2.5 m above the bottom plate. An excavation bench (1800 m away from the structural opening in the tunnel) and a lining trolley (716 m away from the structural opening in the tunnel) were flushed out of the hole owing to the huge water pressure. Regrettably, a local villager doing cleaning work approximately 100 m away from the structural opening died after an unsuccessful emergency rescue attempt. Further, two workers died on the scene. The water inrush lasted approximately 40 min until the situation smoothed favorably for ample rescue operations.

#### 3.2. Rescue Operation

Rescue operations were undertaken immediately by an investigation agency working collaboratively with the government of Guizhou province, construction and supervision units, firefighters, and medical staff, as shown in Figure 4. Twenty-four-hour on-duty monitoring was implemented, and the structural opening of the tunnel was closed. In addition, protective facilities and warning signs were installed to avoid secondary disasters.



**Figure 3.** Accident scenes: (a) Water rushing out of structural opening; (b) portable dwellings destroyed by inrushing water; and (c) ventilation machine flushed away by inrush water.

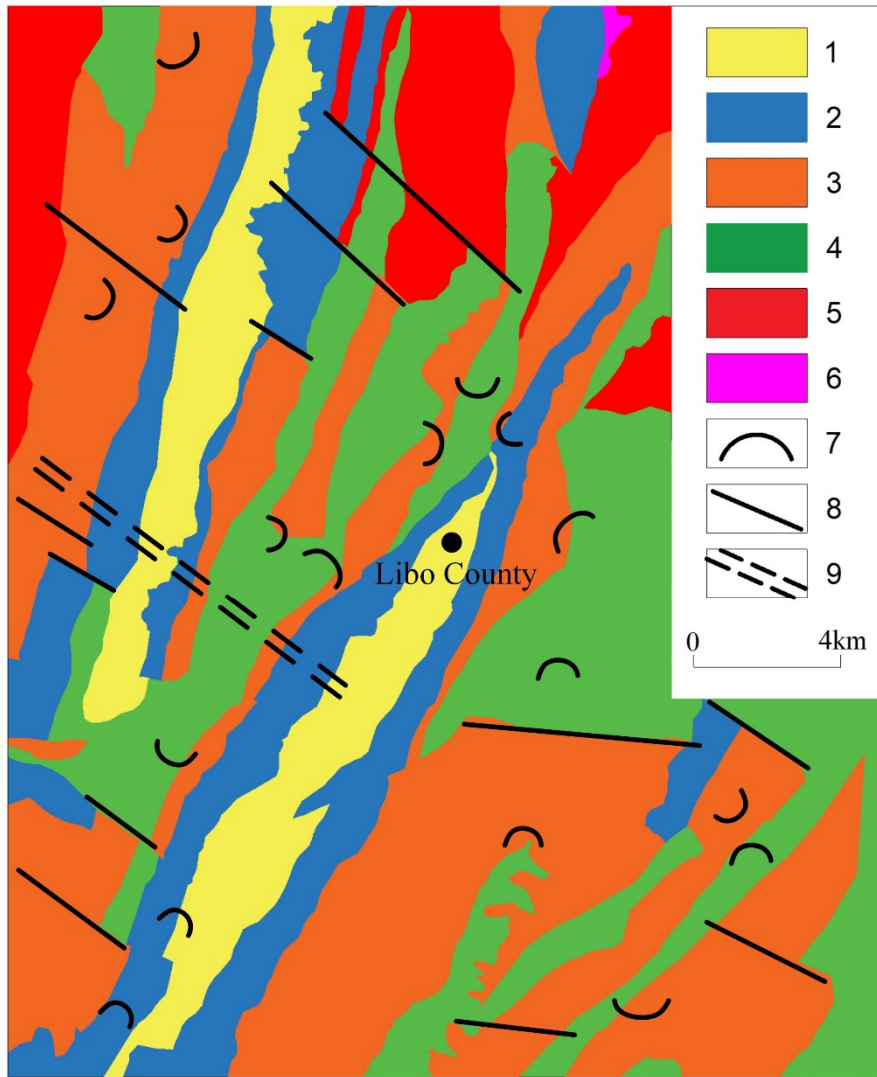


**Figure 4.** Joint rescue activity: (a) Firefighters searching for victims; (b) emergency treatment (Picture source: <http://m.news.cctv.com/2018/06/11/ARTI6F58tT5PonH5KXoex9X5180611.shtml>).

## 4. Discussion

### 4.1. Unfavourable Geological Condition

The incident point is covered by the terrain of karst depression with a buried depth of about 230 m. Figure 5 shows the geological map of Libo County. The tunnel passes through a medium-low mountainous area with peak bushes and low-lying valleys. The site is covered by soft layers of silty clay with average depth of 0–2 m, and the bedrock of Permian Qixia Formation limestone, limestone with intercalation of shale, Carboniferous Mapping Formation limestone, and limestone interlayered with dolomite. Figure 6 shows the sectional view of geological conditions along the tunnel alignment. The incident occurs when excavation in the contact zone of limestone and limestone interlayered with shale, which is water softened and is easy to disintegrate when exposed to air.



1. shale, siltstone, and limestone; 2. limestone, argillaceous limestone, shale, and sandstone; 3. limestone and dolomite; 4. limestone, shale, and siltstone; 5. carbonate rock, sandstone, and basal conglomerate; 6. cambrian dolomite; 7. cave; 8. fault; 9. tunnel

Figure 5. Geological map of Libo County (recreated based on [39]).

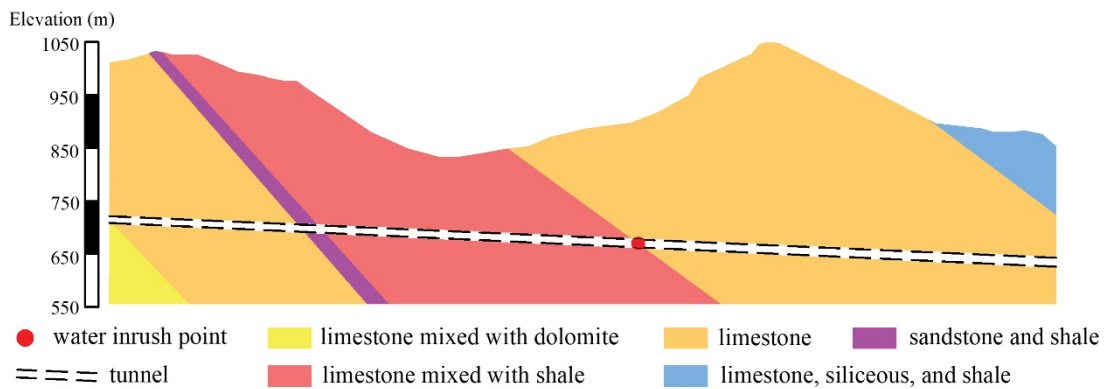


Figure 6. Sectional view of geological profiles for incident point.

Moreover, karst is greatly developed on the site and karst caves are sporadically encountered during construction process. Usually, the developments of karst are widely encountered during excavation,

which often induce several hazards and a variety of engineering construction accidents. In terms of the effect of fissures on the corrosion of karst caves, it is found that the faults and fractures play an important role in karst corrosion [40,41]. The analyses indicated that the karst fractures increase the area of contact between water and carbonate rock, which helps to increase the limestone erosion, and has a clear effect on the stabilization of tunnel rock. The adverse geological formation of the site is believed to be the origin of the water inrush incident in Libo County.

#### 4.2. Inrushing Mechanism

Further investigations were conducted to analyze the water inrush disaster in this project and results showed that the mineralogical composition, physical, mechanical, and hydrological conditions of rock played a key role in this event. Based on aforementioned analysis on inrush materials and alteration conditions, the inrush mechanism in the Chaoyang tunnel can be summarized as follow:

When the tunnel excavated the altered zone (limestone with intercalation of shale), the main equilibrium of materials and mechanics in the altered area was suddenly collapsed. On one hand, once the free surface of the karst cave was disturbed, the leakage pressure dramatically increased through a very short time. Under the influence of groundwater leakage pressure and gravity, the karst cave instantaneously collapsed, resulting in a large-scale inrush event. High pressure groundwater flew through the tunnel along weak frames and structural components. Then, the flowing water constantly eroded and transported the loose soil in the altered area. On the other hand, tunnel excavation has caused disturbances and redistribution of pressure in the surrounding rock masses. In this project, the tunnel passed through altered limestone layer, which represents a common soluble rock that provide the place for groundwater flow and migration. This type of rock with highly soluble rock is likely to induce water inrush [42,43]. At the same time, the construction of tunnel in karst caverns broke the balance of the original ecology. Moreover, the level of groundwater was high which resulted in a series of geological hazards, including water inflow and inrush. This groundwater played a major role as a driving force for the water inrush process. The condition became even worse owing to groundwater recharged by surface water body, which is detailed in the following sections.

#### 4.3. Hydraulic Conductivity

A reservoir with a storage capacity of 125 thousand  $\text{m}^3$  was found 1 km away (in northeast direction) from the tunnel during the investigation. The observations show that at 1:00 p.m. on the day of the accident, the water level was stable at the mid-height of the reservoir. Nevertheless, the reservoir level decreased dramatically the next day and reached one fifth of the reservoir. This means the decrease of surface water body of about 37.5 thousand  $\text{m}^3$  occurred in one day, thereby indicating a possible connection between karst water and reservoir water body. It is believed that the latter may communicate with the karstic water system through karst shaft. The karst water system can be dynamically adjusted by the infiltration of atmospheric precipitation and flow of underground water especially in rainy seasons. The severity of the incident was further aggravated owing to the linkage between underground water and surface water system. Consequently, pressure is released centrally in the form of water inrush and mud discharge after the critical state is reached.

On the other hand, the permeability and porosity of the fissure region increased the erosion of the fissure and thus, collapsed the karst. Based on tunnel investigations department and at the same time the reference of the previous literature, the porosity of the fracture core region ranges from 20% to 35% [40].

#### 4.4. Heavy Precipitations

The rainfall water was considered as another significant cause of the water inrush incident. The monthly average rainfall in Libo County reached its peak (244.45 mm) in June, as shown in Figure 7a. The precipitations in May 2016 and 2017 measured 222.3 mm and 184.8 mm, respectively, according to the information provided by the local weather bureau. However, statistical records for the same period

but 2018 reveal that the precipitation reached 250.4 mm, which is more than twice as the monthly average rainfall of 103.7 mm. Moreover, Libo County was stricken by a heavy rainfall on 4 June. The precipitation reached the astonishing value of 53.6 mm, as shown in Figure 7b. The intense rainfall is one of the critical triggering factors since it resulted in the increase of surface water which became the main recharge source of underground karst water system. Consequently, the unfavorable situation was further aggravated because of the triggering factor of heavy rainfall and tunnel excavation. Figure 8 shows a schematic cause-and-effect diagram of the water inrush incident.

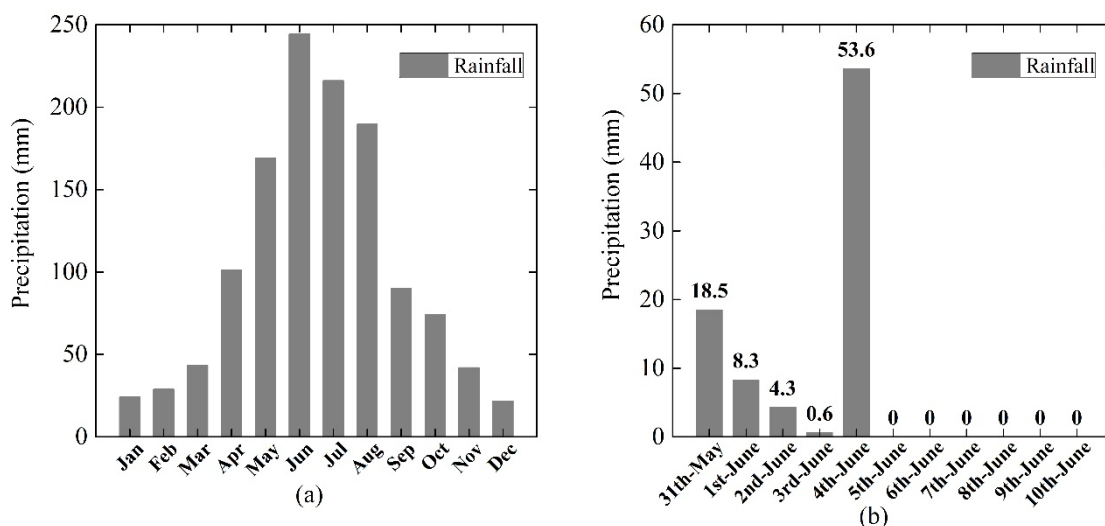


Figure 7. (a) Average monthly rainfall in Libo County. (b) Rainfall in Libo prior to the incident.

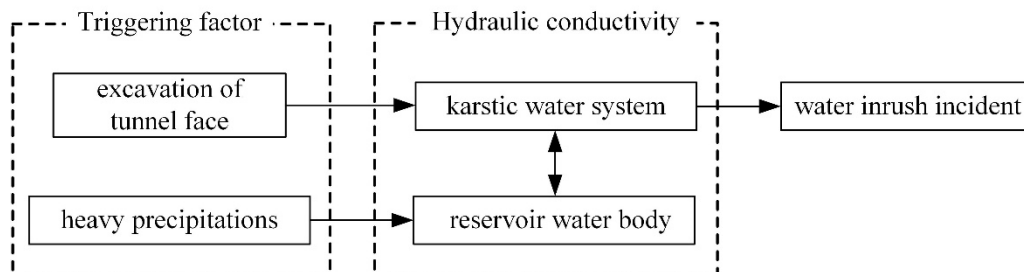


Figure 8. Schematic flowchart of water inrush incident.

#### 4.5. Recommendations

To shorten distances and avoid large ramps, tunnels are increasingly built in mountainous areas. However, many geohazards and fatal incidents occurred during the construction of these mountain tunnels; in particular, in unfavorable geological conditions. The incidents resulted in considerable human and economic losses each year in China. To mitigate these adverse effects, both technical and non-technical countermeasures should be employed to prevent water inrushes:

1. Studying the mechanisms of water inrushes is relatively arduous given the complexity of the interaction between the different fields involved, including engineering geology, rock mechanics, hydrogeology, weather conditions, and human factors. In this case, geographical information system (GIS) and artificial neural networks can be used to evaluate the vulnerability of the karst water [44]; further, fuzzy mathematic methods [45–48] and risk management approaches [49,50] can be employed to assess the water inrush risk in different sections. These methods should be utilized for the risk classification of constructions located in disaster-prone areas.
2. It is well acknowledged that a clear understanding of the engineering geology is the premise of a secure construction. However, it is difficult to predict the ground conditions ahead of the tunnel

face effectively, owing to both technical means and human factors. Therefore, comprehensive composite forecast methods, rather than single geological forecast methods, are recommended for a synthetic analysis. These forecast methods include tunnel seismic prediction, ground-penetrating radar, and the transient electromagnetic method [51].

3. Monitoring systems play an important role in mitigating damages of water inrush incidents. Reliable monitoring methods should be cost-effective; in particular, during constructions in karst geological conditions. A fiber Bragg grating (FBG)-based system can be used to forecast water inrush disasters by monitoring multiple parameters such as the displacement, strain, seepage pressure, and temperature simultaneously [52]. Moreover, workers should regularly conduct evacuation practices, and effective evacuation routes should be planned beforehand, thereby reducing casualties in similar incidents in the future.

## 5. Conclusions

This paper is a report on a water inrush incident that occurred on 10 June 2018 in Guizhou, China. Based on the preliminary investigation and analysis, the following conclusions can be drawn:

1. A large-scale water inrush accident of about 57 thousand m<sup>3</sup> of water occurred in Libo County, thereby resulting in three casualties. The water level reached a maximal height of 2.5 m above the bottom plate. The inrush incident lasted for approximately 40 min. An excavation bench and lining trolley in the tunnel were flushed out of the hole owing to the huge water pressure.
2. The aggregated effect of (i) the karst geology which exhibits well-developed caves, (ii) hydraulic conductivity of the karst water system and surface water body, and (iii) heavy precipitations prior to the incident, thereby contributing to huge human and material resource losses.
3. The assessment of the risk grade should be conducted in water inrush-prone areas. Effective monitoring methods should be utilized to foresee the danger. Methods for advanced predictions should be operated comprehensively to completely detect the geological conditions of the tunnel face front. In addition, self-protection skills should be taught to the workers.

**Author Contributions:** This paper represents a result of collaborative teamwork. Y.-S.X. developed the concept and supervised the work; N.Z. drafted the manuscript; Q.Z. collected the data and revised the manuscript; and K.E. provided constructive suggestions and revised the manuscript. The four authors contributed equally to this work. All authors have read and agreed to the published version of the manuscript.

**Funding:** This work was supported by the Innovative Research Funding of the Science and Technology Commission of Shanghai Municipality (Grant No. 18DZ1201102), the Research Funding of Shantou University for New Faculty Member (Grant No. NTF19024-2019), the National Nature Science Foundation of China (NSFC) (Grant No. 41672259). The financial supports are gratefully acknowledged.

**Conflicts of Interest:** The authors declare no conflict of interest.

## References

1. Tan, J.S.; Shen, S.L.; Zhou, A.N.; Wang, Z.N.; Lyu, H.M. Laboratory evaluation of long-term sealing behaviors of two water-swelling materials for shield tunnel gasket. *Constr. Build. Mater.* **2020**, *249*, 118711. [[CrossRef](#)]
2. Wu, H.N.; Shen, S.L.; Yang, J. Identification of tunnel settlement caused by land subsidence in soft deposit of Shanghai. *J. Perform. Constr. Facil. ASCE* **2017**, *31*, 04017092. [[CrossRef](#)]
3. Wang, Z.N.; Shen, S.L.; Zhou, A.N.; Xu, Y.S. Experimental evaluation of aging characteristics of EPDM as a sealant for undersea shield tunnels. *J. Mater. Civ. Eng. ASCE* **2020**, (in press). [[CrossRef](#)]
4. Lyu, H.M.; Shen, S.L.; Zhou, A.N.; Yang, J. Perspectives for flood risk assessment and management for mega-city metro system. *Tunn. Undergr. Space Technol.* **2019**, *84*, 31–44. [[CrossRef](#)]
5. Elbaz, K.; Shen, S.L.; Sun, W.J.; Yin, Z.Y.; Zhou, A.N. Prediction model of shield performance during tunneling via incorporating improved Particle Swarm Optimization into ANFIS. *IEEE Access* **2020**, *8*, 39659–39671. [[CrossRef](#)]
6. Liu, X.X.; Shen, S.L.; Xu, Y.S.; Yin, Z.Y. Analytical approach for time-dependent groundwater inflow into shield tunnel face in confined aquifer. *Int. J. Numer. Anal. Methods Geomech.* **2018**, *42*, 655–673. [[CrossRef](#)]

7. Wu, H.N.; Shen, S.L.; Yang, J.; Zhou, A.N. Soil-tunnel interaction modelling for shield tunnels considering shearing dislocation in longitudinal joints. *Tunn. Undergr. Space Technol.* **2018**, *78*, 168–177. [[CrossRef](#)]
8. Yang, C.; Shen, S.L.; Hou, D.W.; Liao, S.M.; Yuan, D.J. Material properties of the seal gasket for shield tunnels: a review. *Constr. Build. Mater.* **2018**, *191*, 877–890. [[CrossRef](#)]
9. Liu, X.X.; Shen, S.L.; Zhou, A.N.; Xu, Y.S. Evaluation of foam conditioning effect on groundwater inflow at tunnel cutting face. *Int. J. Numer. Anal. Methods Geomech.* **2019**, *43*, 463–481. [[CrossRef](#)]
10. Shen, S.L.; Wu, Y.X.; Xu, Y.S.; Hino, T.; Wu, H.N. Evaluation of hydraulic parameters from pumping tests of multi-aquifers with vertical leakage Tianjin. *Comput. Geotech.* **2015**, *68*, 196–207. [[CrossRef](#)]
11. Shen, S.L.; Wu, Y.X.; Misra, A. Calculation of head difference at two sides of a cut-off barrier during excavation dewatering. *Comput. Geotech.* **2017**, *91*, 192–202. [[CrossRef](#)]
12. Wu, H.N.; Shen, S.L.; Chen, R.P.; Zhou, A.N. Three-dimensional numerical modelling on localised leakage in segmental lining of shield tunnels. *Comput. Geotech.* **2020**, *122*, 103549. [[CrossRef](#)]
13. Wu, Y.X.; Shen, J.S.; Cheng, W.C.; Hino, T. Semi-analytical solution to pumping test data with barrier, wellbore storage, and partial penetration effects. *Eng. Geol.* **2017**, *226*, 44–51. [[CrossRef](#)]
14. Wu, Y.X.; Shen, S.L.; Yuan, D.J. Characteristics of dewatering induced drawdown curve under blocking effect of retaining wall in aquifer. *J. Hydrol.* **2016**, *539*, 554–566. [[CrossRef](#)]
15. Wu, Y.X.; Lyu, H.M.; Han, J.; Shen, S.L. Case study: Dewatering-induced building settlement around a deep excavation in the soft deposit of Tianjin, China. *J. Geotech. Geoenviron. Eng. ASCE* **2019**, *145*. [[CrossRef](#)]
16. Wu, Y.X.; Lyu, H.M.; Shen, S.L.; Zhou, A.N. A three-dimensional fluid-solid coupled numerical modeling of the barrier leakage below the excavation surface due to dewatering. *Hydrogeol. J.* **2020**, *28*. (in press). [[CrossRef](#)]
17. Wu, Y.X.; Shen, S.L.; Lyu, H.M.; Zhou, A.N. Analyses of leakage effect of waterproof curtain during excavation dewatering. *J. Hydrol.* **2020**, *583*, 124582. [[CrossRef](#)]
18. Xu, Y.S.; Yan, X.X.; Shen, S.L.; Zhou, A.N. Experimental investigation on the blocking of groundwater seepage from a waterproof curtain during pumped dewatering in an excavation. *Hydrogeol. J.* **2019**, *27*, 2659–2672. [[CrossRef](#)]
19. Wang, X.W.; Yang, T.L.; Xu, Y.S.; Shen, S.L. Evaluation of optimized depth of waterproof curtain to mitigate negative impacts during dewatering. *J. Hydrol.* **2019**, *577*, 123969. [[CrossRef](#)]
20. Elbaz, K.; Shen, S.L.; Zhou, A.N.; Yin, Z.Y.; Lyu, H.M. Prediction of disc cutter life during shield tunneling with AI via incorporation of genetic algorithm into GMDH-type neural network. In *Engineering*; Elsevier: Amsterdam, The Netherlands, 2020; Volume 8. (in press)
21. Tan, Y.; Lu, Y. Forensic diagnosis of a leaking accident during excavation. *J. Perform. Constr. Facil. ASCE* **2017**, *31*, 04017061. [[CrossRef](#)]
22. Ren, D.J.; Shen, S.L.; Arulrajah, A.; Wu, H.N. Evaluation of ground loss ratio with moving trajectories induced in double-O-tube (DOT) tunnelling. *Can. Geotech. J.* **2018**, *55*, 894–902. [[CrossRef](#)]
23. Gao, M.Y.; Zhang, N.; Shen, S.L.; Zhou, A. Real-time dynamic regulation of earth pressure for shield tunneling using GRU deep learning method. *IEEE Access* **2020**, *8*. (in press). [[CrossRef](#)]
24. Zhang, N.; Shen, J.S.; Zhou, A.N.; Arulrajah, A. Tunneling induced geohazards in mylonite rock faults with rich groundwater: A case study in Guangzhou. *Tunn. Undergr. Space Technol.* **2018**, *74*, 262–272. [[CrossRef](#)]
25. Zhang, N.; Shen, S.L.; Zhou, A.N.; Chen, J. A brief report on March 21, 2019 explosions of a chemical factory in Xiangshui, China. *Process Saf. Prog.* **2019**, *38*, e12060. [[CrossRef](#)]
26. Yin, Z.Y.; Jin, Y.F.; Shen, J.S.; Hicher, P.Y. Optimization techniques for identifying soil parameters in geotechnical engineering: Comparative study and enhancement. *Int. J. Numer. Anal. Methods Geomech.* **2018**, *42*, 70–94. [[CrossRef](#)]
27. Lin, S.S.; Shen, S.L.; Zhou, A.N.; Lyu, H.M. Sustainable development and environmental restoration in Lake Erhai, China. *J. Clean. Prod.* **2020**, *258*, 120758. [[CrossRef](#)]
28. Lyu, H.M.; Shen, S.L.; Arulrajah, A. Assessment of geohazards and preventive countermeasures using AHP incorporated with GIS in Lanzhou, China. *Sustainability* **2018**, *10*, 304. [[CrossRef](#)]
29. Atangana Njock, P.G.; Shen, S.L.; Zhou, A.N.; Lyu, H.M. Evaluation of soil liquefaction using AI technology incorporating a coupled ENN/t-SNE model. *Soil Dyn. Earthq. Eng.* **2020**, *130*, 105988. [[CrossRef](#)]
30. Atangana Njock, P.G.; Shen, S.L.; Zhou, A.N.; Lyu, H.M. Data on a coupled ENN/t-SNE model for soil liquefaction evaluation. *Data Brief* **2020**, *30*, 105125. [[CrossRef](#)]

31. Zhang, N.; Shen, S.L.; Zhou, A.N.; Xu, Y.S. Investigation on performance of neural network using quadratic relative error cost function. *IEEE Access* **2019**, *7*, 106642–106652. [[CrossRef](#)]
32. Shen, S.L.; Wang, J.P.; Wu, H.N.; Xu, Y.S. Evaluation of hydraulic conductivity for both marine and deltaic deposits based on piezocone testing. *Ocean Eng.* **2015**, *110*, 174–182. [[CrossRef](#)]
33. Ward, P.J.; Kumm, M.; Lall, U. Flood frequencies and durations and their response to El Niño Southern Oscillation: Global analysis. *J. Hydrol.* **2016**, *539*, 358–378. [[CrossRef](#)]
34. Lyu, H.M.; Sun, W.J.; Shen, S.L.; Arulrajah, A. Flood risk assessment in metro systems of mega-cities using a GIS-based modeling approach. *Sci. Total Environ.* **2018**, *626*, 1012–1025. [[CrossRef](#)] [[PubMed](#)]
35. Lyu, H.M.; Zhou, W.H.; Shen, S.L.; Zhou, A.N. Inundation risk assessment of metro system using AHP and TFN-AHP in Shenzhen. *Sustain. Cities Soc.* **2020**, *57*, 102103. [[CrossRef](#)]
36. Lyu, H.M.; Shen, S.L.; Yang, J.; Yin, Z.Y. Inundation analysis of metro systems with the storm water management model incorporated into a geographical information system: a case study in Shanghai. *Hydrol. Earth Syst. Sci.* **2019**, *23*, 4293–4307. [[CrossRef](#)]
37. Huang, X.J. Influence factors of water bursting and mud bursting of karst tunnels and its countermeasures. *J. Railw. Eng. Soc.* **2013**, *30*, 45–53. (In Chinese) [[CrossRef](#)]
38. Wu, L.; Wan, J.W.; Chen, G.; Zhao, L. Cause of the “8.5” water burst incident at Yesanguan tunnel along the Yi-Wan railway. *Carsologica Sin.* **2009**, *28*, 212–218. (In Chinese) [[CrossRef](#)]
39. Zhang, M.L.; Lin, Y.S.; Ran, J.C.; Chen, H.M. The Characteristics of Karst Caves Development in Libo, Guizhou. *Carsologica Sin.* **2000**, *19*, 13–20. (In Chinese)
40. Zhao, Y.; Wang, F.; Li, C.; Cao, Y.; Tian, H. Study of the Corrosion Characteristics of Tunnel Fissures in a Karst Area in Southwest China. *Geofluids* **2018**, 1–19. [[CrossRef](#)]
41. Elbaz, K.; Shen, S.L.; Cheng, W.C.; Arulrajah, A. Cutter-disc consumption during earth-pressure-balance tunnelling in mixed strata. *Geotech. Eng. ICE Proc.* **2018**, *171*, 363–376. [[CrossRef](#)]
42. Wang, X.T.; Li, S.C.; Xu, Z.H.; Hu, J.; Pan, D.D.; Xue, Y.G. Risk assessment of water inrush in karst tunnels excavation based on normal cloud model. *B Eng. Geol. Environ.* **2019**. [[CrossRef](#)]
43. Elbaz, K.; Shen, S.L.; Zhou, A.N.; Yuan, D.J.; Xu, Y.S. Optimization of EPB shield performance with adaptive neuro-fuzzy inference system and genetic algorithm. *Appl. Sci.* **2019**, *9*, 780. [[CrossRef](#)]
44. Wu, Q.; Xu, H.; Pang, W. GIS and ANN coupling model: an innovative approach to evaluate vulnerability of karst water inrush in coalmines of north China. *Environ. Geol.* **2008**, *54*, 937–943. [[CrossRef](#)]
45. Lyu, H.M.; Shen, S.L.; Yang, J.; Zhou, A.N. Risk assessment of earthquake-triggered geohazards surrounding Wenchuan, China. *Nat. Hazards Rev. ASCE* **2020**, (in press). [[CrossRef](#)]
46. Lyu, H.M.; Sun, W.J.; Shen, S.L.; Zhou, A.N. Risk assessment using a new consulting process in fuzzy AHP. *J. Constr. Eng. Manag. ASCE* **2020**, *146*(3), 04019112. [[CrossRef](#)]
47. Lyu, H.M.; Shen, S.L.; Zhou, A.N.; Yang, J. Risk assessment of mega-city infrastructures related to land subsidence using improved trapezoidal FAHP. *Sci. Total Environ.* **2020**, *717*, 135310. [[CrossRef](#)]
48. Lyu, H.M.; Shen, S.L.; Zhou, A.N.; Zhou, W.H. Flood risk assessment of metro systems in a subsiding environment using the interval FAHP-FCA approach. *Sustain. Cities Soc.* **2019**, *50*, 101682. [[CrossRef](#)]
49. Gallina, V.; Torresan, S.; Critto, A. A review of multi-risk methodologies for natural hazards: Consequences and challenges for a climate change impact assessment. *J. Environ. Manag.* **2016**, *168*, 123–132. [[CrossRef](#)]
50. Marchi, L.; Borga, M.; Preciso, E.; Gaume, E. Characterization of selected extreme flash floods in Europe and implications for flood risk management. *J. Hydrol.* **2010**, *394*, 118–133. [[CrossRef](#)]
51. Zhang, Q.S.; Li, S.C.; Ge, Y.H.; Xu, Z.H.; Liu, R.T. Study on Risk Evaluation Method of Water Inrush and Integrated Geological Prediction Technology in High-Risk Karst Tunnel. In Proceedings of the GeoHunan international conference, Changsha, China, 9 June 2011; pp. 285–291. [[CrossRef](#)]
52. Liu, B.; Li, S.C.; Wang, J.; Sui, Q.M.; Nie, L.C.; Wang, Z.F. Multiplexed FBG Monitoring System for Forecasting Coalmine Water Inrush Disaster. *Adv. Optoelectron.* **2012**, 1–10. [[CrossRef](#)]

